

See discussions, stats, and author profiles for this publication at: <https://www.researchgate.net/publication/50373541>

# Type and Location of Interaction between Hyperbranched Polymers and Liposomes. Relevance to Design of a Potentially Advanced Drug Delivery Nanosystem (aDDnS)

ARTICLE *in* THE JOURNAL OF PHYSICAL CHEMISTRY B · MARCH 2011

Impact Factor: 3.3 · DOI: 10.1021/jp1123458 · Source: PubMed

---

CITATIONS

6

---

READS

28

## 7 AUTHORS, INCLUDING:



**Elena A. Mourelatou**

National and Kapodistrian University of Athens

12 PUBLICATIONS 57 CITATIONS

SEE PROFILE



**Dima Libster**

Hebrew University of Jerusalem

32 PUBLICATIONS 553 CITATIONS

SEE PROFILE



**Sophia Hatziantoniou**

University of Patras

55 PUBLICATIONS 966 CITATIONS

SEE PROFILE

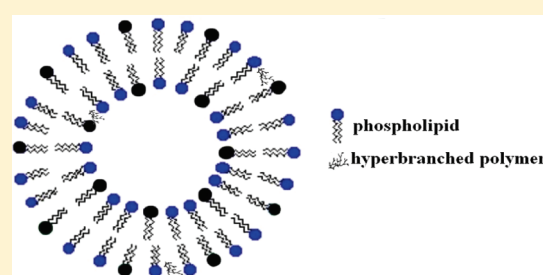
# Type and Location of Interaction between Hyperbranched Polymers and Liposomes. Relevance to Design of a Potentially Advanced Drug Delivery Nanosystem (aDDnS)

Elena A. Mourelatou,<sup>†,⊥</sup> Dima Libster,<sup>‡</sup> Ido Nir,<sup>‡,||</sup> Sophia Hatziantoniou,<sup>†</sup> Abraham Aserin,<sup>‡</sup> Nissim Garti,<sup>‡,§</sup> and Costas Demetzos<sup>\*,†,§</sup>

<sup>†</sup>Department of Pharmaceutical Technology, School of Pharmacy, University of Athens, Panepistimiopolis Zografou, 15771 Athens, Greece

<sup>‡</sup>The Ratner Chair of Chemistry, Casali Institute of Applied Chemistry, The Institute of Chemistry, The Hebrew University of Jerusalem, Edmond J. Safra Campus, Jerusalem 91904, Israel

**ABSTRACT:** Advanced drug delivery nanosystems (aDDnSs) combining liposomal and dendritic materials have only recently appeared in the research field of drug delivery. The nature and localization of the interactions between the components of such systems are not yet fully described. In this study, liposomes are combined with hyperbranched polyesters for the development of new aDDnSs. The polymer–lipid interactions along with their dependence on the polyesters pseudogeneration number and the liposomal lipid composition have been examined. The results indicate that the interaction between the materials takes place in the headgroup region, where H-bonds between the polymers terminal hydroxyls and the phospholipids phosphate moiety are formed. Due to the polymers' compact imperfect structure, which varies with pseudogeneration number, no linear trends are observed with increasing pseudogeneration number. Moreover, it is shown that high percentages of cholesterol in the lipid bilayer affect the penetration of the polymers in the headgroup region.



## INTRODUCTION

In the field of drug delivery, various approaches for the development of new and more effective drug carriers have been implemented. Among the materials used, the lipidic and the polymeric ones have attracted the most attention. A great number of studies have been performed with liposomes and dendrimers as carriers of drug molecules, genetic materials, targeting agents, and/or imaging agents.<sup>1,2</sup> In the past few decades, new classes of drug carriers have emerged, derived from the combination of different kinds of biomaterials. The main motivation for such an approach was the alteration of the pharmacodynamic profile and the improvement of the drugs' therapeutic index. One of these classes comprises carriers produced by the combination of liposomes with dendrimers.<sup>3–5</sup> These carriers were recently characterized as chimeric advanced drug delivery nanosystems (chi-aDDnSs)<sup>6</sup> belonging to the class of modulatory liposomal controlled released systems (MLCRSs),<sup>5</sup> where the dendritic component acts as a modulator of the drugs' release from the carrier. So far the studies performed were focused on the effect of the dendritic material to the encapsulation efficiency of the drug in the carrier and/or the modification of its release from the system. The interactions between the components, specifically between the liposomes and the dendrimers, responsible for the observed results are still unclear.

A relatively young class of dendritic polymers, named hyperbranched polymers (HBPs), has lately attracted much attention

of research and their effectiveness in replacing dendrimers as drug carriers is under study. HBPs are characterized by a high degree of branching, a three-dimensional architecture, and multiple terminal functional units.<sup>7</sup> Compared to dendrimers, they are more polydisperse, due to their random branching and the existence of partially reacted linear repeat units in their structure. However, they are obtained via one-step reactions, through the statistical polymerization of AB<sub>x</sub>-type monomers by means of condensation or addition procedures, which makes them low-cost, easily produced high functional products. Although current advances in research of polymers with highly branched architecture have created opportunities for the development of new drug delivery systems, the research of HBPs as drug carriers is still in its infancy. Several approaches have been performed, including entrapment or non-covalent attachment of drug molecules to HBPs (drug complexes or unimolecular micelles), covalent conjugation of drug molecules to the terminal groups of HBPs, and drug loading in multimolecular micelle cores.<sup>8</sup> So far, no study involving the combination of HBPs and liposomes has been reported.

In this study, polyol hyperbranched polymers have been employed along with liposomes for the preparation of new

**Received:** December 29, 2010

**Revised:** February 8, 2011

**Published:** March 11, 2011

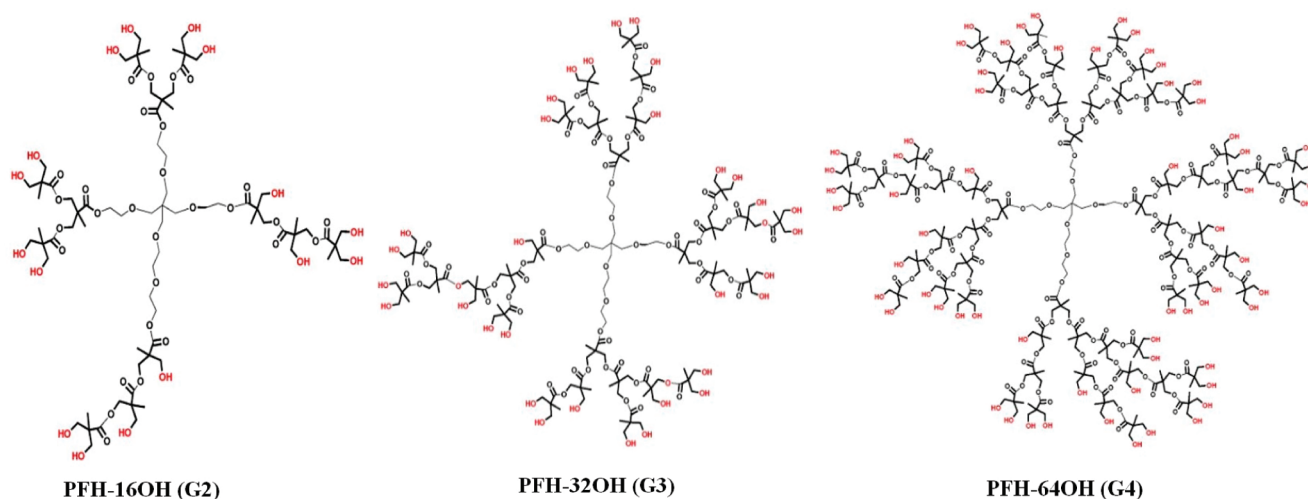


**Figure 1.** G2, G3, and G4 aliphatic polyester HBPs.

chi-aDDnSs. Aliphatic polyester HBPs are prepared from 2,2-dimethylolpropionic acid (bis-MPA) as monomer and a polyol (epoxylated pentaerythritol) as a core. As a result, they have multiple terminal hydroxyl groups, which facilitate their interaction with other proton or acceptor groups through H-bond formation. Three different pseudogenerations of aliphatic polyesters G2, G3, and G4, with 16, 32, and 64 peripheral hydroxyl groups, respectively, have been incorporated in two different liposomal formulations (with and without cholesterol). The main focus of this study is the investigation of the interactions established between HBPs and phospholipids and their dependence on HBPs pseudogeneration number and liposomal lipid composition. The nature of the interaction was characterized with the use of attenuated total reflectance–Fourier transform infrared spectroscopy (ATR-FTIR), pulse generated spin echo–nuclear magnetic resonance (PGSE-NMR), and  $^{31}\text{P}$  NMR. ATR-FTIR technique provides the ability to measure samples in excess water without the use of spectroscopic probes. Detection of H-bond breaking or formation and changes in conformation and/or hydration level can be established through monitoring frequency shifts or bandwidth changes of corresponding bands, thus allowing the localization of molecules binding sites in the bilayer and the identification of possible structural changes induced by the binding process. PGSE-NMR is able to distinguish free molecules from liposome-incorporated ones and has been used for the evaluation of drug encapsulation efficiency.<sup>9</sup>  $^{31}\text{P}$  NMR was employed for examining the changes induced in the phospholipids' headgroup (HG) mobility by the polymers incorporation.

## EXPERIMENTAL METHODS

**Materials.** Hyperbranched aliphatic polyesters were purchased from Sigma-Aldrich. PFH-16OH [ $\text{C}_{75}\text{H}_{128}\text{O}_{45}$ , MW 1749.79, pseudogeneration 2], PFH-32OH [ $\text{C}_{155}\text{H}_{256}\text{O}_{93}$ , MW 3607.64, pseudogeneration 3], and PFH-64OH [ $\text{C}_{315}\text{H}_{512}\text{O}_{189}$ , MW 7323.32, pseudogeneration 4] HBPs are presented in Figure 1. The phospholipids (PLs) used for the liposomal formulations were 1,2-distearoyl-*sn*-glycero-3-phosphocholine (DSPC), 1,2-dipalmitoyl-*sn*-glycero-3-phospho-(1'-*rac*-glycerol) (sodium salt) (DPPG), and cholesterol (( $3\beta$ )-cholest-5-en-3-ol). They were purchased from Avanti Polar Lipids and used without further

purification. All other reagents used were of analytical grade and purchased from Sigma-Aldrich Chemical Co..

**Liposome Preparation.** Two different liposomal formulations have been prepared using the thin-film hydration method, one composed of DSPC/DPPG (70:30 molar ratio) and one of DSPC/cholesterol (65:35). Briefly, appropriate amounts of lipid solutions in organic solvents (chloroform/methanol 1:1) were placed in a round-bottom flask and a thin lipid film was formed by slow removal of the solvents at 40 °C under vacuum using a rotary evaporator. The lipid film was further dried in vacuum overnight to remove any traces of organic solvents. Liposomes were formed during hydration of the lipid film with appropriate volume of citrate buffer (300 mM, pH 4.0) at 70 °C for 1 h, under constant rotation. Large unilamellar vesicles (LUVs) were finally formed with extrusion through polycarbonate membranes of specific pore diameter (400 and 100 nm) under pressure. Liposomal formulations with incorporated HBPs were prepared using the same method, where 5% molar ratio of HBP (PFH-16OH, PFH-32OH, or PFH-64OH) was added each time. The HBPs were incorporated during the thin lipid film formation; specific volume of HBPs methanol solutions was added to the lipid solutions in the round-bottom flask prior to the lipid film formation. The procedure continues as described above until LUV vesicles are formed. All liposomal formulations were stored at 4 °C. The vesicles size and size distribution of empty and polymer-loaded liposomes were measured at 25 °C using photon correlation spectroscopy (PCS) on a Zetasizer 3000 HSA (Malvern Instruments, UK) at a detection angle of 90°.  $\zeta$ -Potential was measured in the same instrument through measurement of the vesicles electrophoretic mobility and the utilization of appropriate algorithms. All measurements were carried out after dilution with a solution of sodium chloride 10 mM.

**ATR-FTIR Measurements.** An Alpha T model spectrometer, equipped with a single reflection diamond ATR sampling module, manufactured by Bruker Optik GmbH (Ettlingen, Germany) was used to record the FTIR spectra. The spectra were recorded with 50 scans, at a temperature range of 25–70 °C and at a wavelength range of 3000 to 400  $\text{cm}^{-1}$ ; a spectral resolution of 2  $\text{cm}^{-1}$  was obtained. For examining the composition and temperature dependence of each band, multi-Gaussian curve fitting was performed to resolve individual bands in the spectra. The peaks were analyzed in terms of peak wavenumber ( $\text{cm}^{-1}$ ), width ( $\text{cm}^{-1}$ ),

**Table 1.** Size, Polydispersity Index (PI), and  $\zeta$ -Potential of All Liposomal Formulations

liposomal formulations	size (nm)	PI	$\zeta$ -potential (mV)
DSPC/DPPG (70:30)	140.1 $\pm$ 1.5	0.197 $\pm$ 0.010	−64.6 $\pm$ 10.2
DSPC/DPPG/PFH-16OH (66.7:28.3:5)	133.5 $\pm$ 4.0	0.227 $\pm$ 0.020	−65.5 $\pm$ 7.0
DSPC/DPPG/PFH-32OH (66.7:28.3:5)	155.6 $\pm$ 2.6	0.235 $\pm$ 0.025	−42.3 $\pm$ 1.5
DSPC/DPPG/PFH-64OH (66.7:28.3:5)	157.5 $\pm$ 2.3	0.260 $\pm$ 0.027	−43.0 $\pm$ 8.5
DSPC/Chol (65:35)	124.2 $\pm$ 0.2	0.101 $\pm$ 0.007	−0.8 $\pm$ 0.7
DSPC/Chol/PFH-16OH (61.8:33.2:5)	121.3 $\pm$ 0.5	0.066 $\pm$ 0.014	−0.3 $\pm$ 0.7
DSPC/Chol/PFH-32OH (61.8:33.2:5)	119.8 $\pm$ 0.1	0.066 $\pm$ 0.006	−0.3 $\pm$ 1.2
DSPC/Chol/PFH-64OH (61.8:33.2:5)	125.6 $\pm$ 0.8	0.086 $\pm$ 0.032	0.9 $\pm$ 0.4

**Table 2.** Assignment of ATR-FTIR Bands to Group Vibration Modes

functional group, assignment	wavenumber (cm <sup>−1</sup> )
PO <sub>2</sub> <sup>−</sup> symmetric stretching ( $\nu_s(\text{PO}_2^-)$ )	1100–1076
PO <sub>2</sub> <sup>−</sup> asymmetric stretching ( $\nu_{as}(\text{PO}_2^-)$ )	1250–1220
chain CH <sub>2</sub> symmetric stretching ( $\nu_s(\text{CH}_2)$ )	2865–2845
chain CH <sub>2</sub> asymmetric stretching ( $\nu_{as}(\text{CH}_2)$ )	2935–2915
CN <sup>+</sup> (CH <sub>3</sub> ) <sub>3</sub> asymmetric stretching ( $\nu_{as}(\text{CN}^+(\text{CH}_3)_3)$ )	≈970
C–O(–H) stretching ( $\nu(\text{C–O})$ )	≈1045

and relative integrated area percentages (%). The collected data were evaluated using as reference samples liposomes without incorporated polymers as well as polymers solutions in citrate buffer 300 mM and as background medium citrate buffer pH 4.0. Spectra analysis and curve fitting was performed with ORIGIN 8.0.

**PGSE-NMR Measurements.** A Bruker DRX-400 spectrometer was used with a BGU II gradient amplifier unit and a 5 mm BBI probe equipped with a z-gradient coil, providing a z-gradient strength ( $g$ ) of up to 55 G cm<sup>−1</sup> and a Bruker AVII 500 spectrometer equipped with GREAT 1/10 gradients and a 5 mm BBI probe with a z-gradient coil with a maximum gradient strength of 0.536 T m<sup>−1</sup>. The self-diffusion (SD) coefficients were determined using pulsed field gradient stimulated spin echo (PFG-SSE).<sup>10,11</sup> In this work, we used bipolar gradient pulses as described by Wu et al.<sup>12</sup> to reduce the eddy-current effects. Experiments were carried out by varying  $g$  and keeping all other timing parameters constant. Gradient pulses of 1–4 ms and intergradient delays between 0.07 and 1 s were used in order to achieve a decay curve that decayed most of the way but not completely to zero in order to optimize the accuracy of the diffusion measurement. The spectrum was processed by a Fourier transform in the acquisition ( $t_2$ ) dimension and by a Levenberg–Marquardt<sup>13,14</sup> fit to decaying Gaussians, supplied with the Bruker TOPSPIN software, to the gradient ramp evolution ( $g$ ) dimension. <sup>1</sup>H-HRMAS and diffusion MAS experiments were carried out on the 500 MHz spectrometer using an HR-MAS probe equipped with a magic-angle gradient using the same pulse sequences and parameters as for the regular liquid-state probes. <sup>31</sup>P NMR spectra were obtained for static or slowly spinning (20 Hz) samples. The spectra were acquired with 320 scans, 30° pulse, and 3.6 s repetition time. The total acquisition time for each spectrum was approximately 20 min.

## RESULTS

**Liposome Preparations.** For the two different liposomal formulations prepared (DSPC/DPPG and DSPC/cholesterol), the size distribution (mean diameter and polydispersity index)

and  $\zeta$ -potential were measured and the results are presented in Table 1. DSPC/DPPG liposomes are slightly larger compared to those containing cholesterol and have wider size distributions as revealed by the PI values. All DSPC/DPPG liposomal formulations exhibit negative  $\zeta$ -potential values attributed to the incorporation of the negatively charged DPPG phospholipid. The  $\zeta$ -potential values of DSPC/cholesterol liposomes showed that these formulations have no surface charge as expected since all lipids used for this preparation were neutral. Incorporation of HBPs in DSPC/DPPG liposomes resulted in slight changes of the liposomes size and an increase of the PI values, while only HBP G3 and G4 incorporation caused a shift of the  $\zeta$ -potential to less negative values. For DSPC/cholesterol liposomes, all parameters remained unchanged upon polymer incorporation.

**ATR-FTIR Measurements.** ATR-FTIR allows the differentiation between the different regions of a lipid bilayer (Table 2). The packing and structure of the acyl chain region in the lipid bilayer are mainly monitored through the symmetric and asymmetric CH<sub>2</sub> stretching vibrations.<sup>15</sup> The frequencies and bandwidths depend on the conformational order and mobility of the acyl chains and can be useful in monitoring the phase transition of the lipid bilayer from gel to liquid crystalline state. Above the transition temperature ( $T_m$ ) of the lipid mixture, a shift of CH<sub>2</sub> frequencies to higher wavenumbers (due to the introduction of gauche conformers), a decrease in intensity, and an increased bandwidth can be observed.<sup>16</sup> No alteration is expected if the incorporated molecules do not penetrate in the hydrocarbon chain region. Moreover, information about the level of hydration and other interactions in the HG region can be extracted from the symmetric and asymmetric vibrations of the phosphate groups.<sup>17</sup> Additionally to the vibrations of the phosphate moiety, the asymmetric stretching vibration of the choline group (<sup>+</sup>N(CH<sub>3</sub>)<sub>3</sub>) was also studied. Changes in the structure and/or hydration of the bilayers water–lipid interface can be observed in the PLs carbonyl (C=O) vibration band.<sup>16</sup> Unfortunately, in this case the existence of multiple carbonyls in the structure of HBPs made the study of the interfacial region of the bilayer via C=O vibration impossible. Finally, information about



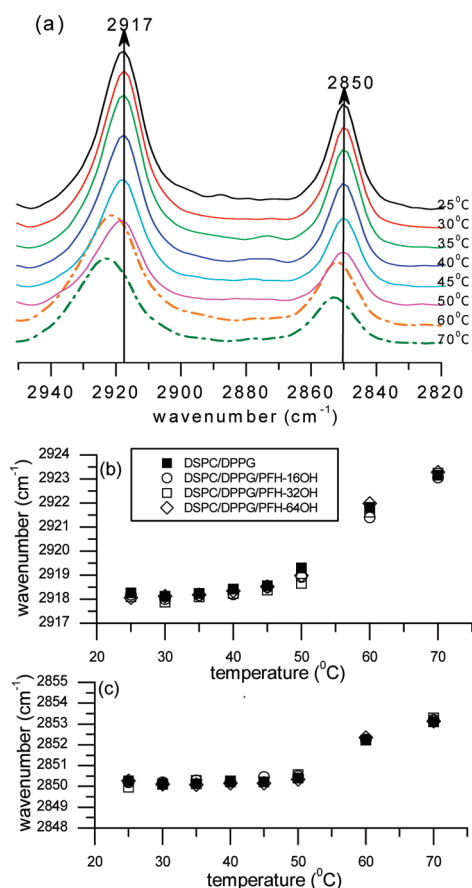


**Figure 2.** (a) ATR-FTIR spectra of the CH<sub>2</sub> stretching bands for DSPC/DPPG liposomes with increasing temperature. (b) CH<sub>2</sub> asymmetric stretching via temperature. (c) CH<sub>2</sub> symmetric stretching via temperature.

the structural changes induced to HBPs after liposome incorporation has been gathered from frequency alterations of the terminal hydroxyl stretching vibration [C–O(–H)].<sup>18</sup>

From ATR-FTIR spectra analysis it is evident that addition of HBPs in DSPC/DPPG liposomal formulations has no perturbing effect in the acyl chain region. The transition occurs around 50 °C (Figure 2a), reflected by a shift to higher wavenumbers of both asymmetric (Figure 2b) and symmetric (Figure 2c) bands. These upward shifts are correlated with lipid tails disordering at temperatures above 50 °C.<sup>16</sup> As shown in Figure 2b,c, only minor effects in the  $\nu_s$  and  $\nu_{as}$  stretching vibrations of CH<sub>2</sub> groups can be observed upon polymer incorporation. This is expected since the polymers polar nature should prevent them from penetrating in the hydrophobic core of the lipid bilayer.

The possible interactions of the polymers with the PLs HGs in both liposomal formulations were first assessed through analysis of the spectra area attributed to the phosphate moiety stretching vibrations (Figure 3). Generally, the phosphate groups are sterically and electronically more exposed and thus able to interact through H-bonding with other molecules.

The PO<sub>2</sub><sup>−</sup> asymmetric stretching is indicative of the degree of hydration in the polar HG region of the bilayer. With increasing temperature, a red shift can be observed in all examined samples, thus suggesting the increase of HG hydration accompanying the transition from gel to liquid crystalline phase.<sup>16,19–21</sup> In the DSPC/DPPG liposomal formulation, HBPs incorporation resulted in a

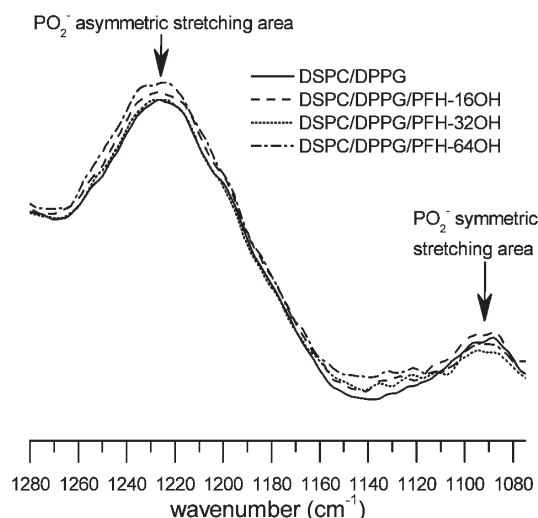


**Figure 3.** ATR-FTIR spectra of the PO<sub>2</sub><sup>−</sup> stretching area in DSPC/DPPG liposomes with and without incorporated HBPs at 25 ± 2 °C.

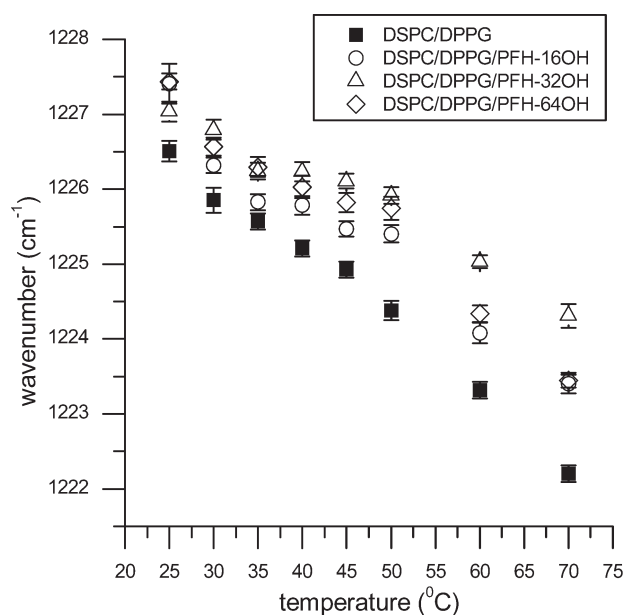


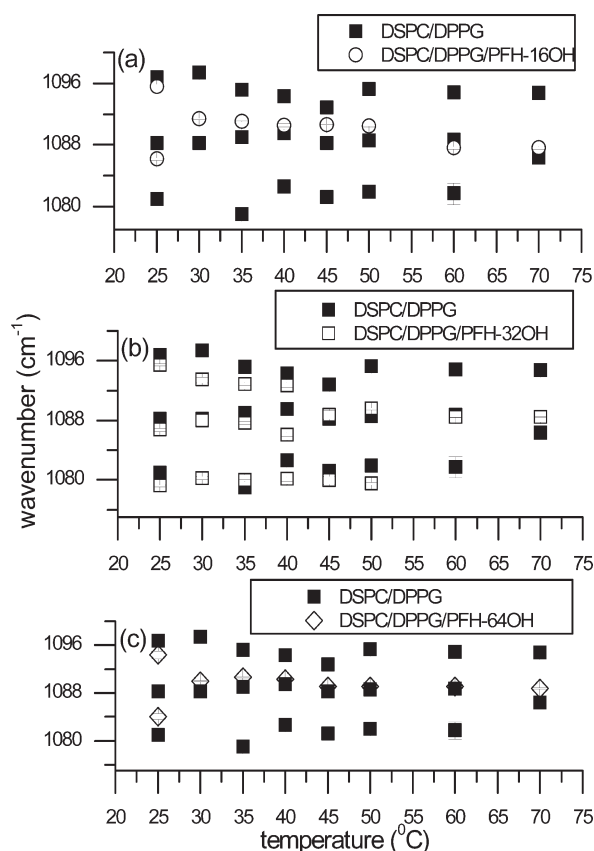
**Figure 4.** Temperature dependence of the PO<sub>2</sub><sup>−</sup> asymmetric stretching for DSPC/DPPG formulations.

shift of the PO<sub>2</sub><sup>−</sup> asymmetric stretching toward higher values (Figure 4). This blue shift could be attributed to the relative dehydration caused by the polymer incorporation, which is more pronounced above the  $T_m$ , especially for G3 polymer incorporation.

In the case of the symmetric stretching of the phosphate moiety, after curve fitting three underlying components can be distinguished in the DSPC/DPPG liposomal formulation (Table 3). Each one of these components can be attributed to subpopulations of PO<sub>2</sub><sup>−</sup> groups located in a different environment; the low-frequency component indicates H-bonded (with water molecules) groups, the high-frequency component indicates free groups, while the middle-frequency component indicates groups participating in intermolecular interactions. It should be remarked that for liposomes without incorporated HBPs the H-bonded PO<sub>2</sub><sup>−</sup> groups dominate over the free groups, thus indicating that the polar HG region is in a

Table 3.  $\text{PO}_2^-$  Symmetric Stretching Vibration Parameters at 25 °C

liposomal formulations	components								
	1			2			3		
	wavenumber ( $\text{cm}^{-1}$ )	width ( $\text{cm}^{-1}$ )	area (%)	wavenumber ( $\text{cm}^{-1}$ )	width ( $\text{cm}^{-1}$ )	area (%)	wavenumber ( $\text{cm}^{-1}$ )	width ( $\text{cm}^{-1}$ )	area (%)
DSPC/DPPG	1096.71 $\pm$ 0.15	6.64 $\pm$ 0.42	11.2	1088.20 $\pm$ 0.12	8.38 $\pm$ 0.57	57.1	1080.92 $\pm$ 0.12	4.98 $\pm$ 0.28	31.7
DSPC/DPPG/PFH-16OH	1095.59 $\pm$ 0.22	13.49 $\pm$ 0.88	75.9	1086.18 $\pm$ 0.16	6.50 $\pm$ 0.31	24.1	—	—	—
DSPC/DPPG/PFH-32OH	1095.44 $\pm$ 0.12	7.20 $\pm$ 0.41	41.4	1086.73 $\pm$ 0.23	9.05 $\pm$ 0.66	54.2	1079.23 $\pm$ 0.23	4.81 $\pm$ 0.39	4.5
DSPC/DPPG/PFH-64OH	1094.37 $\pm$ 0.62	14.16 $\pm$ 1.00	78.0	1084.05 $\pm$ 0.50	8.79 $\pm$ 0.71	22.0	—	—	—
DSPC/Chol	1096.82 $\pm$ 0.53	8.13 $\pm$ 0.75	29.4	1087.12 $\pm$ 0.58	11.67 $\pm$ 0.94	70.6	—	—	—
DSPC/Chol/PFH-16OH	1091.82 $\pm$ 0.28	4.40 $\pm$ 1.00	4.7	1086.53 $\pm$ 0.58	13.02 $\pm$ 1.25	95.3	—	—	—
DSPC/Chol/PFH-32OH	1097.9 $\pm$ 0.15	5.86 $\pm$ 0.25	19.8	1088.12 $\pm$ 0.14	11.43 $\pm$ 0.34	80.2	—	—	—
DSPC/Chol/PFH-64OH	1097.64 $\pm$ 0.29	8.85 $\pm$ 0.96	43.5	1087.05 $\pm$ 0.27	8.75 $\pm$ 0.59	56.5	—	—	—

Figure 5. Temperature dependence of the  $\text{PO}_2^-$  symmetric stretching of liposomes with incorporated (a) G2 polymer, (b) G3 polymer, and (c) G4 polymer.

well-hydrated state. Incorporation of HBPs G2 and G4 results in the loss of the low-frequency component and the decrease in frequency of the other two components, which is more pronounced for polymer G4. Additionally, the relative ratio of free over H-bonded groups changes in favor of the free ones. These are all indicative of the HBP–PL interaction, which leads to the loosening of bonding of the phosphate moiety with water molecules, the replacement of water molecules by HBP molecules, and the subsequent formation of new H-bonds with different strengths. In the case of G3 polymer incorporation,

Table 4.  $\text{PO}_2^-$  Asymmetric Stretching Vibration Parameters for DSPC/Cholesterol Liposomes at 25 °C

liposomal formulations	wavenumber ( $\text{cm}^{-1}$ )	width ( $\text{cm}^{-1}$ )
DSPC/Chol	1228.19 $\pm$ 0.13	35.93 $\pm$ 0.85
DSPC/Chol/PFH-16OH	1228.27 $\pm$ 0.12	36.61 $\pm$ 0.93
DSPC/Chol/PFH-32OH	1228.14 $\pm$ 0.10	40.04 $\pm$ 0.94
DSPC/Chol/PFH-64OH	1227.65 $\pm$ 0.12	39.13 $\pm$ 1.11

the number of components remains unchanged, but again the peaks' wavenumber and the percentage of H-bonded groups decrease, suggesting a less pronounced but still evident interaction of the polymer with the HGs.

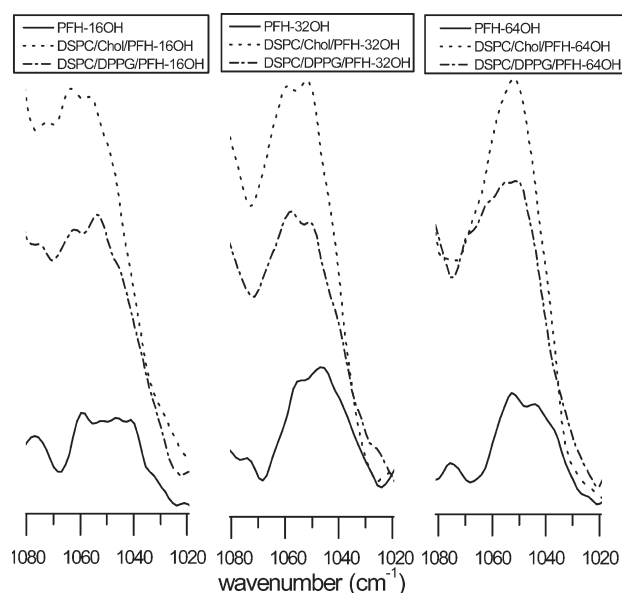
With increasing temperature, liposomes with incorporated G2 and G4 polymers exhibit only one population of phosphate groups (Figure 5). The high- and low-frequency components no longer appear, suggesting that all the phosphate groups are participating in a network of intermolecular H-bonds with the water and the polymer molecules.

In the case of G3 incorporation, the three different components of the phosphate groups were detected with increasing temperature up to 40 °C, but they are still downshifted compared to DSPC/DPPG liposomes. From 45 °C and above, the number of components is decreased and only after the transition temperature one component is evident. This indicates that the polymer–phosphate group interaction remains and becomes even more intense in the liquid crystalline state.

On the contrary, incorporation of polymers in liposomes containing high percentages of cholesterol showed no significant change in the  $\text{PO}_2^-$  asymmetric stretching and thus on the hydration level of the HG region (Table 4). For the  $\text{PO}_2^-$  symmetric stretching two subpopulations (free and H-bonded) of  $\text{PO}_2^-$  groups can be distinguished, the number of which remains unaffected by the polymers incorporation (Table 3). Only the polymer of the lowest pseudogeneration (G2) caused a significant downshift of the peak suggesting polymer–HG interaction, attributed to its smaller size. It should be noted that incorporation of all HBPs does not change the distribution of free and H-bonded subpopulations of  $\text{PO}_2^-$  groups. The above observations could lead to the conclusion that polymers in DSPC/cholesterol formulation are localized in the liposomes' outer surface and cannot penetrate deeper into the polar HG region.

**Table 5.**  $^+N-(CH_3)_3$  Asymmetric Stretching Vibration Parameters at  $25 \pm 2^\circ C$ 

liposomal formulations	wavenumber ( $cm^{-1}$ )	width ( $cm^{-1}$ )
DSPC/DPPG	$971.71 \pm 0.22$	$6.77 \pm 0.78$
DSPC/DPPG/PFH-16OH	$972.20 \pm 0.39$	$7.26 \pm 0.73$
DSPC/DPPG/PFH-32OH	$972.23 \pm 0.36$	$7.33 \pm 1.25$
DSPC/DPPG/PFH-64OH	$973.75 \pm 0.94$	$3.82 \pm 1.95$
DSPC/Chol	$972.20 \pm 0.04$	$10.36 \pm 0.14$
DSPC/Chol/PFH-16OH	$972.18 \pm 0.08$	$7.88 \pm 0.30$
DSPC/Chol/PFH-32OH	$971.05 \pm 0.22$	$6.76 \pm 0.64$
DSPC/Chol/PFH-64OH	$968.75 \pm 0.61$	$8.33 \pm 0.70$

**Figure 6.** ATR-FTIR spectra of the C–O(–H) band for liposomes and polymers in citrate buffer.

To complete the study of the bilayers HG region, the C–N asymmetric stretching in the  $^+N-(CH_3)_3$  moiety, which is sensitive to dipolar interactions, was assessed. Since the most probable sites to accept an H-bond are the oxygen atoms connected to the phosphorus, modifications in the choline moiety vibrations would indirectly reflect the effect of polymer incorporation in the polar HG region. Shifts in the  $\nu_{as}(CN^+-(CH_3)_3)$  frequency can be related to conformational changes of the choline induced by the intercalation of molecules (i.e., water, sugars) between the phosphate and the choline groups.<sup>22</sup> Additionally, despite the apolar nature of this group, the methyl and methylene groups of the choline moiety have the ability to form H-bonds with donor–acceptor groups, such as water molecules, as a result of their being acidified by the electron-withdrawing influence of the positively charged nitrogen atom.<sup>23</sup> In this case, the formation of a C–H···OH bond results in the shortening of the C–H bond and the blue shift of the  $\nu_{as}(CN^+(CH_3)_3)$  stretching.

The analysis of the C–N asymmetric band (Table 5) indicates that once more the effect of HBP incorporation is dependent on both the pseudogeneration number and lipid composition. Specifically, incorporation of G2 and G3 HBPs in DSPC/DPPG liposomes resulted in only minor changes in the  $\nu_{as}(CN^+(CH_3)_3)$  stretching vibrations, whereas G4 incorporation caused a significant increase. This suggests that the bulkier

G4 HBP, having increased number of functional hydroxyl groups, can establish H-bonds with the choline group and/or change its conformation due to its intercalation between the phosphate and the choline moiety. For DSPC/cholesterol formulations, again G2 and G3 polymers have minor effect on  $\nu_{as}(CN^+(CH_3)_3)$  stretching vibration, while G4 polymer causes a downshift in the corresponding wavenumber. This indicates weakening of the C–H···OH interactions.

Additionally to the regions in the IR spectra attributed to the PLs, the C–O(–H) stretching of the HBPs terminal groups was also examined (Figure 6). The study of C–O(–H) vibrations offers advantages such as that there is no substantial band broadening and intensity changes when H-bonds occur, while discrete H-bond species can be identified.

It should be mentioned that features appearing at 1070 and 1058  $cm^{-1}$  for DSPC/DPPG liposomes and at 1063  $cm^{-1}$  for DSPC/cholesterol liposomes are assigned to the ester C–O–C symmetric stretching vibration.<sup>24</sup>

From the results presented in Table 6, two different subpopulations of C–O(–H) groups are present in the HBPs structure. In all three HBPs, the H-bonded groups are dominant.

Incorporation of HBPs in DSPC/DPPG liposomes leads to a blue shift of the C–O(–H) stretching vibration. The more pronounced shift is observed in the case of the G2 and G4 polymer, where a change in the relative percentages of free and H-bonded groups is also detected. In the case of G3 polymer the shift is less pronounced, since the H-bonded groups are still the dominant ones. Data collected at different temperatures (below and above the transition temperature of the liposomal lipid bilayer) indicate that even at high temperatures (above the  $T_m$ ) the polymers still remain inside the bilayer of DSPC/DPPG liposomes (Figure 7).

The above results lead us to suggest HBPs relocation from the more hydrophilic environment of the aqueous medium to the less hydrophilic HG region of the liposomal bilayer. When the polymers are located in the less hydrophilic environment of the lipid bilayer, the network of H-bonds is rearranged and perhaps they acquire a more compact structure where most of the terminal hydroxyl groups are no longer accessible for H-bonding with the PLs phosphate groups or water molecules.

Incorporation of HBPs in DSPC/Cholesterol liposomes induced only minor effects in the frequency of the C–O(–H) stretching vibrations, suggesting that the polymers are not fully inserted into the bilayer.

**PGSE-NMR Measurements.**  $^1H$  NMR spectra obtained with static methods are usually very broad, since the time scale is too slow to average out the anisotropic interactions, and do not allow the assignment of all chemically significant groups or the study of the dynamic of membranes to be obtained through relaxation experiments.<sup>25</sup> In order to average the inhomogeneous and anisotropic interactions present in large unilamellar liposomes (LUVs), high-resolution magic angle spinning (HR-MAS) technique was employed, while the resolution was further increased by raising the temperature at 60  $^\circ C$  (above the transition temperature of the lipid mixture) and the spinning speed at 12 kHz. Using these conditions, the line widths of the NMR signals were sensibly narrowed and the isotropic chemical shifts of all protons in the polar HG as well as the glycerol backbone of the PLs can be resolved.

PGSE-NMR is based upon the measurement of the diffusion coefficient of all different species in a multicomponent system simultaneously, with a nonperturbing in situ manner.<sup>26</sup> From the

Table 6. C–O(–H) Stretching Vibration Parameters for Free and Liposome Incorporated HBPs

sample	components					
	1			2		
	wavenumber (cm <sup>-1</sup> )	width (cm <sup>-1</sup> )	area (%)	wavenumber (cm <sup>-1</sup> )	width (cm <sup>-1</sup> )	area (%)
PFH-16OH	1046.26 ± 0.53	5.00 ± 1.15	41.9	1040.42 ± 0.44	5.77 ± 0.49	58.1
DSPC/DPPG/PFH-16OH	1053.99 ± 0.13	12.09 ± 0.75	87.7	1043.64 ± 0.24	6.05 ± 0.73	12.3
DSPC/Chol/PFH-16OH	1047.28 ± 0.11	4.70 ± 0.27	27.6	1040.81 ± 0.14	7.85 ± 0.47	72.4
PFH-32OH	1049.51 ± 0.26	5.69 ± 0.49	38.4	1041.50 ± 0.83	9.31 ± 2.89	61.6
DSPC/DPPG/PFH-32OH	1052.83 ± 0.26	5.23 ± 0.55	36.1	1044.99 ± 0.29	8.19 ± 1.23	63.9
DSPC/Chol/PFH-32OH	1050.03 ± 0.55	6.01 ± 0.82	50.9	1042.09 ± 0.68	6.78 ± 1.42	49.1
PFH-64OH	1043.70 ± 0.27	5.00 ± 0.75	22.7	1037.79 ± 0.57	8.59 ± 0.89	77.3
DSPC/DPPG/PFH-64OH	1050.05 ± 0.20	8.63 ± 0.23	100	—	—	—
DSPC/Chol/PFH-64OH	1042.73 ± 0.61	6.89 ± 3.08	63.7	1037.71 ± 0.69	5.26 ± 0.69	36.3

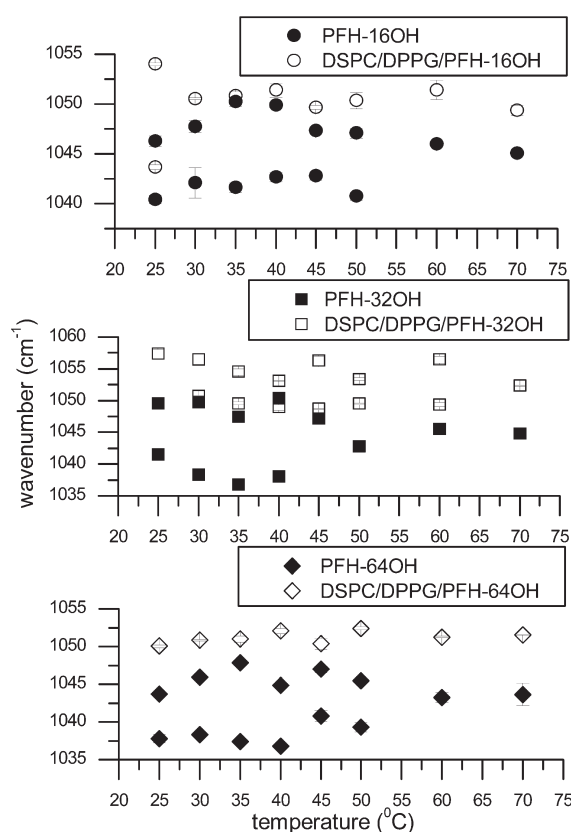


Figure 7. Temperature dependence of the polymers C–O(–H) stretching of DSPC/DPPG liposomes with incorporated (a) G2 polymer, (b) G3 polymer, and (c) G4 polymer.

PGSE-NMR spectra obtained at 60 °C, the diffusion coefficients of liposomes and free HBPs were calculated. HBPs exhibit faster diffusion rates on the order of  $10^{-9}$ – $10^{-10}$  m<sup>2</sup>/s compared to liposomes, where the diffusion coefficient is of the order of  $10^{-11}$  m<sup>2</sup>/s (Table 7). In the case of liposomes incorporating HBPs, it can be observed that the polymers diffusion rate decreases and their diffusion coefficient acquires values of the same order as for liposomes. This suggests the diffusion of the polymers together with liposomes as one complex. The fact that no free HBP molecules are observed in these systems indicate that all of the HBP molecules are incorporated in the liposomes and the observed

Table 7. Diffusion Coefficient Values for HBPs and DSPC/DPPG Liposomal Formulations Extracted from <sup>1</sup>H SD-NMR Spectra at 60 °C

system	composition	component	diffusion coeff (m <sup>2</sup> /s)
liposomes	DSPC/DPPG	PL	$2.34 \times 10^{-11}$
	DSPC/DPPG/PFH-16OH	PL	$2.39 \times 10^{-11}$
		polymer	$2.76 \times 10^{-11}$
	DSPC/DPPG/PFH-32OH	PL	$8.46 \times 10^{-12}$
		polymer	$1.68 \times 10^{-11}$
	DSPC/DPPG/PFH-64OH	PL	$1.61 \times 10^{-11}$
HBPs		polymer	$1.96 \times 10^{-11}$
	PFH-16OH	polymer	$2.32 \times 10^{-9}$
	PFH-32OH	polymer	$1.56 \times 10^{-10}$
	PFH-64OH	polymer	$2.38 \times 10^{-9}$

phenomena cannot be attributed to the encapsulation of the polymers in the confined space of the liposomal aqueous cavity.

The above observations are in accordance to the ATR-FTIR results, which indicated the interaction of the HBPs with the PLs HG.

**<sup>31</sup>P NMR Measurements.** <sup>31</sup>P NMR spectra of DSPC/DPPG liposomes with and without the incorporated HBPs acquired at 25 °C are shown in Figure 8. All the spectra have the typical type of line shape found in LUV phospholipid vesicles below the transition temperature which is attributed to the chemical shift anisotropy of the phosphate phosphorus.<sup>27</sup> The peaks are broad, asymmetric, and centered around 0 ppm, whereas on heating the samples above the transition temperature (60 °C) sharp spectra were obtained for all liposomal formulations (spectra not shown).

In this study the parameter of interest was the line width at half-height of the peak ( $\Delta\nu_{1/2}$ ), which is directly related to the allowed motion in the phosphate group region of the polar HG.<sup>27</sup> Differences in the  $\Delta\nu_{1/2}$  arise from differences in the dipolar interactions and can indicate interaction of the HBPs with the phosphate moiety.

Measurements of the  $\Delta\nu_{1/2}$  values in all liposomal formulations indicate an increase of width with increasing pseudogeneration number of incorporated hyperbranched polymer, from 3 to 7 ppm. This is related to a decrease in the local mobility of the HG or a reorientation of the phosphate moiety. This effect is attributed to the interaction of the polymers with the phosphate group either by direct bonding or through intercalation of the polymers in the HG



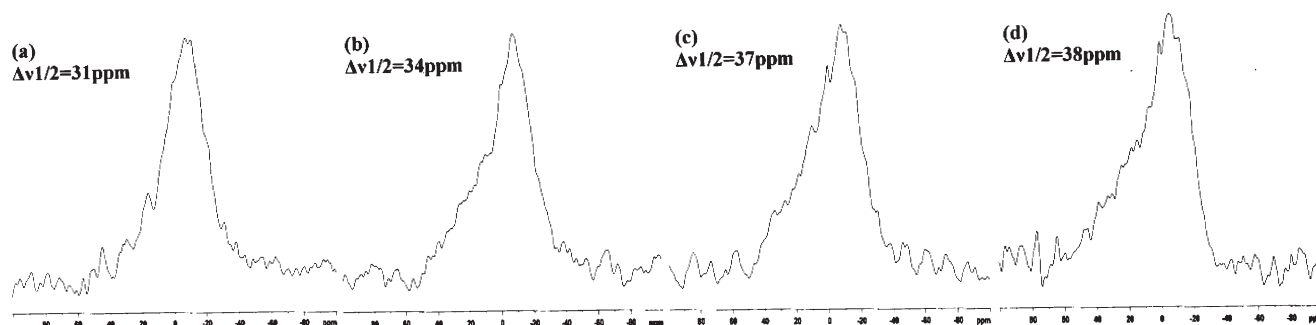


**Figure 8.**  $^{31}\text{P}$  NMR spectra of (a) DSPC/DPPG, (b) DSPC/DPPG/PFH-16OH, (c) DSPC/DPPG/PFH-32OH, and (d) DSPC/DPPG/PFH-64OH liposomes.

region resulting in alterations of the hydration level and/or polar HG conformation, as also indicated by the ATR-FTIR studies.

## DISCUSSION

ATR-FTIR spectra analysis of liposomes containing HBPs of different pseudogeneration number has provided information regarding the site of interaction between the lipidic and dendritic components. As it was expected, owing to the polar nature of the polymers, the penetration of these molecules deep into the hydrocarbon chain region of the lipid bilayer is restricted. The polymers seem mainly to interact with the phosphate moiety and this interaction depends on the pseudogeneration number of the polymer as well as the composition of the lipid bilayer. Generally, it could be concluded that HBPs compete with water molecules, which act as a net repulsing force opposing the polymers intercalation into the lipid bilayer. The successful polymer incorporation requires the rearrangement of the inter- and intramolecular H-bonding network already existing in the HG region, established between the PLs and the water molecules as well as between adjacent phospholipid and perhaps the replacement of water molecules bound to this region. Consequently, the mobility of the PLs HG decreases, as revealed by the  $^{31}\text{P}$  NMR measurements, due to the intercalation of the bulky polymer molecules.

Interestingly, it has been observed that in liposomes containing high percentages of cholesterol the HBPs incorporation in the HG region is being restricted. No severe shifts could be observed in either the stretchings of the HG region or the C–O(H) stretching of the HBPs. This phenomenon is related to the effect of high cholesterol concentrations on the ordering and conformation of the PL molecules in the lipid bilayer. It is well-known in the literature that cholesterol decreases the liposomes' membrane permeability, broadens the gel to liquid phase transition, and modulates the acyl chain order in both the gel and liquid crystalline state.<sup>28</sup> Cholesterol also affects the conformation of the HG region in the bilayer, and at high percentages (30–50%) it increases the hydrophobicity of the interfacial region, a factor that influences the incorporation of molecules in the lipid bilayer.<sup>29</sup> This action is obtained through the disruption of the intermolecular phospholipid interactions and the establishment of a new network of H-bonds. The cholesterol hydroxyl group can act as either a H-bond donor or acceptor and thus form three different kinds of H-bonds with (i) an oxygen atom in the phospholipid molecule ( $\text{OH}\cdots\text{O}$  bond); (ii) a water molecule, thus creating a water bridge connecting cholesterol with phospholipids; or (iii) a methyl

group of the choline moiety ( $\text{CH}\cdots\text{O}$  bond).<sup>30</sup> As a result, the orientation of the plane constituted by the phosphate and the choline groups becomes parallel to the bilayer normal with a slightly inward direction, so that the choline group approaches the cholesterol hydroxyl group. This conformation and the H-bond network formed are related to the inability of the polymers to strongly interact with DSPC/cholesterol liposomes. It is possible that the disruption of the coexisting H-bond network in the HG region by the HBP molecules is energetically unfavorable.

Furthermore, the pseudogeneration number of the HBPs is also influencing the interactions presented in the final system. From the results obtained in this study, no linear relationship between the pseudogeneration number and the strength of the interaction can be established. Surprisingly, the HBPs of the lower and higher pseudogeneration number (G2 and G4) seem to exhibit the strongest interactions with the HG region. These phenomena can be attributed to the specific structure that the HBPs have. Analytically, computational and experimental studies performed on HBPs of different pseudogenerations have shown the formation of a network of several kinds of inter- and intramolecular H-bonds with different strengths, between the hydroxyl, carbonyl, and carboxylic groups.<sup>18,31</sup> This bond network results in the acquisition of a rather compact structure, leading to the steric isolation of several functional groups. The kind of H-bonds formed as well as their relative strength is different with increasing pseudogeneration number. No comparative study of the H-bond network and the final compactness of the polymers structure has been performed so far for the three HBPs used in this study, so we cannot have a clear image of the differences observed with increasing pseudogeneration number. Nevertheless, we have concluded that the pseudogeneration number dependence of the HBP–PL interaction is generally a resultant of the relative contributions of three main parameters: (1) number of functional hydroxyl and/or carbonyl groups, (2) size, and (3) compactness of structure as defined from the specific inter- and intra-H-bond network formed.

## CONCLUSIONS

New chi-aDDnSs have been prepared by the combination of lipidic and dendritic materials, and ATR-FTIR and NMR studies were performed for the evaluation of the incorporation of HBPs in liposomes. From the measurements performed, the site of the interaction between the two different components was identified and its dependence on pseudogeneration number and lipid composition has been established.

The measurements revealed that the HBP–PL interaction takes place at the polar lipid HG region, where polymer incorporation results in the dehydration of the HG and the decrease of the HGs' mobility. The insertion of polymers in the lipid bilayer seems to be an energetically driven process that in order to be successful the rearrangement of H-bond network has to be favored. Further insight in the exact phenomena occurring during HBPs incorporation could be obtained through thermodynamic studies. Finally, for the designing of such chi-aDDnSs, increased cholesterol concentrations should be avoided, whereas the HBPs pseudogeneration number, and thus the size and number of terminal hydroxyl groups, are also parameters that should be taken into account.

The findings of this study can prove helpful to rationally design new and innovative liposomal drug carriers for bioactive molecules by combining dendritic and liposomal technologies.

## AUTHOR INFORMATION

### Corresponding Author

\*E-mail: demetzos@pharm.uoa.gr.

### Author Contributions

<sup>§</sup>These authors contributed equally to this work.

### Current Address

<sup>||</sup>The Israel Institute for Biological Research, P.O.B.19, Ness-Ziona, 74100, Israel.

### Notes

<sup>⊥</sup>This work is a part of Ph.D thesis of Elena Mourelatou.

## ACKNOWLEDGMENT

We thank COST—European Cooperation in Science and Technology (TD0802) for financial support, Pharmaserve Lilly S.ACI (Greece) for supporting our research, and Maria Zervou, Ph.D., Institute of Organic and Pharmaceutical Chemistry, National Hellenic Research Foundation, for her contribution.

## REFERENCES

- (1) Banerjee, R. J. *Biomater. Appl.* **2001**, *16*, 3.
- (2) Tomalia, D. A.; Reyna, L. A.; Svenson, S. *Biochem. Soc. Trans.* **2007**, *35*, 61.
- (3) Gardikis, K.; Hatziantoniou, S.; Bucos, M.; Fessas, D.; Signorelli, M.; Felekis, T.; Zervou, M.; Screttas, G. C.; Steele, R. B.; Ionov, M.; Micha-Screttas, M.; Klajnert, B.; Bryszewska, M.; Demetzos, C. *J. Pharm. Sci.* **2010**, *99*, 3561.
- (4) Khopade, A. J.; Caruso, F.; Tripathi, P.; Nagaich, S.; Jain, N. K. *Int. J. Pharm.* **2002**, *232*, 157.
- (5) Papagiannaros, A.; Dimas, K.; Papaioannou, G. T.; Demetzos, C. *Int. J. Pharm.* **2005**, *302*, 29.
- (6) Gardikis, K.; Tsimplouli, C.; Dimas, K.; Micha-Screttas, M.; Demetzos, C. *Int. J. Pharm.* **2010**, *402*, 231.
- (7) Hult, A.; Johansson, M.; Malmström, E. Hyperbranched Polymers. In *Branched Polymers II*; Springer: New York, 1999; p 1.
- (8) Zhou, Y.; Huang, W.; Liu, J.; Zhu, X.; Yan, D. *Adv. Mater.* **2010**, *22*, 4567.
- (9) Momot, K. I.; Kuchel, P. W. *Concepts Magn Reson Part A* **2003**, *19A*, 51.
- (10) Garti, N.; Avrahami, M.; Aserin, A. *J. Colloid Interface Sci.* **2006**, *299*, 352.
- (11) Libster, D.; Aserin, A.; Garti, N. *J. Colloid Interface Sci.* **2006**, *302*, 322.
- (12) Wu, D. H.; Chen, A. D.; Johnson, C. S. *J Magn Reson, Ser. A* **1995**, *115*, 260.
- (13) Marquardt, D. W. *J. Soc. Ind. Appl. Math.* **1963**, *11*, 431.
- (14) Levenberg, K. *Q. Appl. Math.* **1944**, *2*, 164.
- (15) Biruss, B.; Dietl, R.; Valenta, C. *Chem. Phys. Lipids* **2007**, *148*, 84.
- (16) Lee, D. C.; Chapman, D. *Biosci. Rep.* **1986**, *6*, 235.
- (17) Arrondo, J. L. R.; Gopi, F. M.; Macarulla, J. M. *Biochim. Biophys. Acta (BBA)—Lipids Lipid Metab.* **1984**, *794*, 165.
- (18) Zagar, E.; Grdadolnik, J. *J. Mol. Struct.* **2003**, *658*, 143.
- (19) Cong, W.; Liu, Q.; Liang, Q.; Wang, Y.; Luo, G. *Biophys. Chem.* **2009**, *143*, 154.
- (20) Cies Mlik-Boczula, K.; Szwed, J.; Jaszczyszyn, A.; Gasiorowski, K.; Koll, A. *J. Phys. Chem. B* **2009**, *113*, 15495.
- (21) Kwon, K. O.; Kim, M. J.; Abe, M.; Ishinomori, T.; Ogino, K. *Langmuir* **1994**, *10*, 1415.
- (22) Cacela, C.; Hinch, D. K. *Biophys. J.* **2006**, *90*, 2831.
- (23) Hinch, D. K.; Popova, A. V.; Cacela, C.; Liu, A. L. Effects of Sugars on the Stability and Structure of Lipid Membranes During Drying. In *Advances in Planar Lipid Bilayers and Liposomes*; Academic Press: New York, 2006; Chapter 6, Vol. 3; p 189.
- (24) Okamura, E.; Umemura, J.; Takenaka, T. *Biochim. Biophys. Acta (BBA)—Biomembr.* **1990**, *1025*, 94.
- (25) Cruciani, O.; Mannina, L.; Sobolev, A.; Cametti, C.; Segre, A. *Molecules* **2006**, *11*, 334.
- (26) Griffiths, P. C.; Cheung, A. Y. F.; Davies, J. A.; Paul, A.; Tipples, C. N.; Winnington, A. L. *Magn. Reson. Chem.* **2002**, *40*, S40.
- (27) Cullis, P. R.; De Kruffy, B.; Richards, R. E. *Biochim. Biophys. Acta (BBA)—Biomembr.* **1976**, *426*, 433.
- (28) Fowler Bush, S.; Levin, H.; Levin, I. W. *Chem. Phys. Lipids* **1980**, *27*, 101.
- (29) Mohammed, A. R.; Weston, N.; Coombes, A. G. A.; Fitzgerald, M.; Perrie, Y. *Int. J. Pharm.* **2004**, *285*, 23.
- (30) Pandit, S. A.; Bostick, D.; Berkowitz, M. L. *Biophys. J.* **2004**, *86*, 1345.
- (31) Tanis, I.; Tragoudaras, D.; Karatasos, K.; Anastasiadis, S. H. *J. Phys. Chem. B* **2009**, *113*, 5356.